Cell Reports, Volume *39*

Supplemental information

Baricitinib attenuates the proinflammatory phase of COVID-19 driven by lung-infiltrating monocytes

Brian Dobosh, Keivan Zandi, Diego Moncada Giraldo, Shu Ling Goh, Kathryn Musall, Milagros Aldeco, Julia LeCher, Vincent D. Giacalone, Junkai Yang, Devon J. Eddins, Manoj Bhasin, Eliver Ghosn, Vikas Sukhatme, Raymond F. Schinazi, and Rabindra Tirouvanziam

A

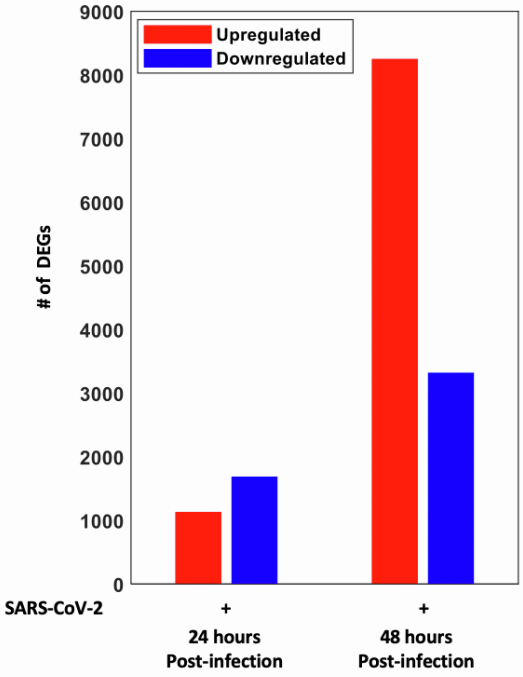
Upregulated
Downregulated
# of DEGs
9000
8000
7000
6000
5000
4000
3000
2000
1000
0
SARS-CoV-2
+
+
24 hours
Post-infection
48 hours
Post-infection

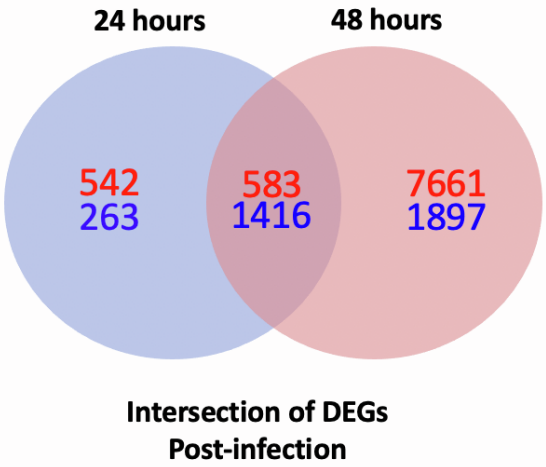
24 hours
48 hours
542
263
583
1416
7661
1897
Intersection of DEGs
Post-infection

B

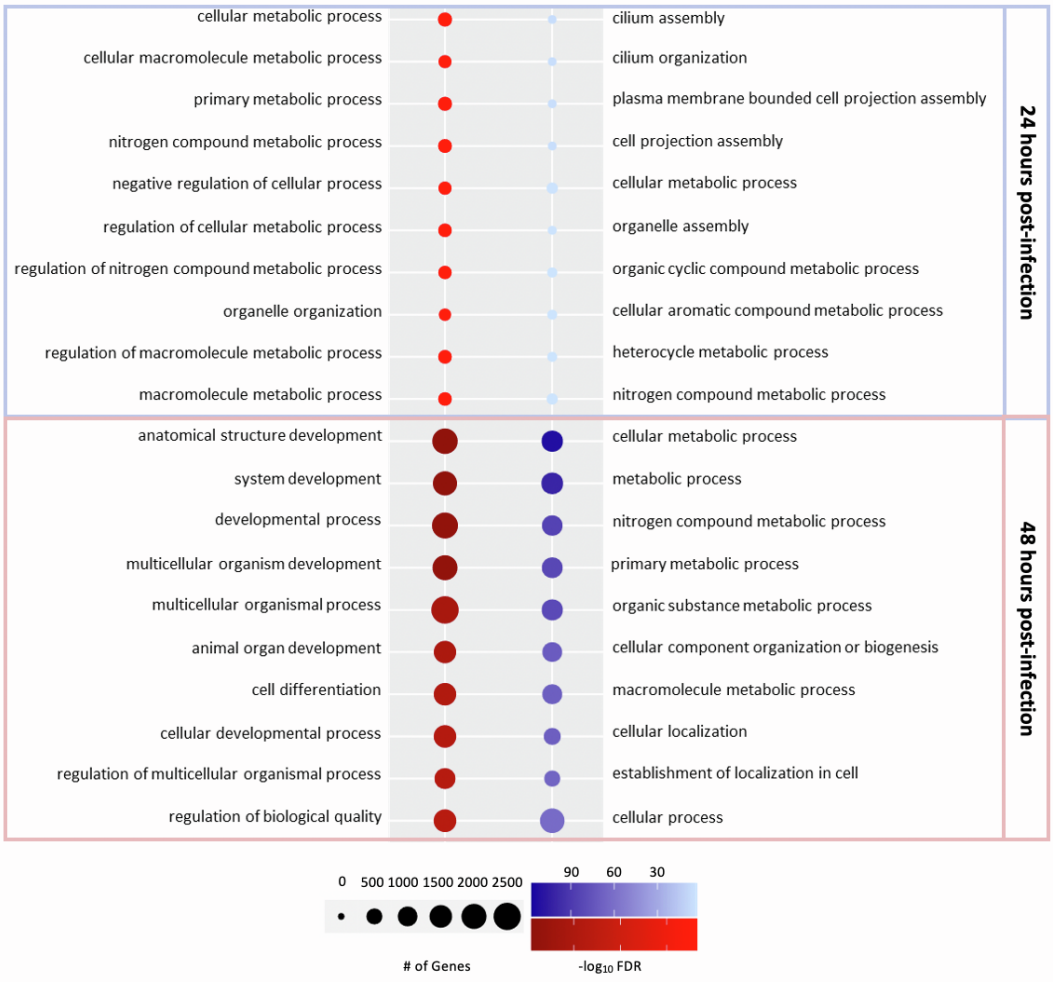
cellular metabolic process
cellular macromolecule metabolic process
primary metabolic process
nitrogen compound metabolic process
negative regulation of cellular process
regulation of cellular metabolic process
regulation of nitrogen compound metabolic process
organelle organization
regulation of macromolecule metabolic process
macromolecule metabolic process
cilium assembly
cilium organization
plasma membrane bounded cell projection assembly
cell projection assembly
cellular metabolic process
organelle assembly
organic cyclic compound metabolic process
cellular aromatic compound metabolic process
heterocycle metabolic process
nitrogen compound metabolic process
24 hours post-infection
anatomical structure development
system development
developmental process
multicellular organism development
multicellular organismal process
animal organ development
cell differentiation
cellular developmental process
regulation of multicellular organismal process
regulation of biological quality
cellular metabolic process
metabolic process
nitrogen compound metabolic process
primary metabolic process
organic substance metabolic process
cellular component organization or biogenesis
macromolecule metabolic process
cellular localization
establishment of localization in cell
cellular process
48 hours post-infection
0 500 1000 1500 2000 2500
# of Genes
90 60 30
-log10 FDR

Supplementary Figure 1. Related to Figure 2. (A) Number of upregulated and downregulated DEGs from the RNA-seq data (n=3 biological replicates) of HLE-ALI cells infected with SARS-CoV-2 for either 24 or 48 hrs. **(B)** GO processes enriched in HLE-ALI cells at either 24 or 48 hrs post-infection with SARS-CoV-2. GO terms were generated using uniquely DEGs between the two conditions.

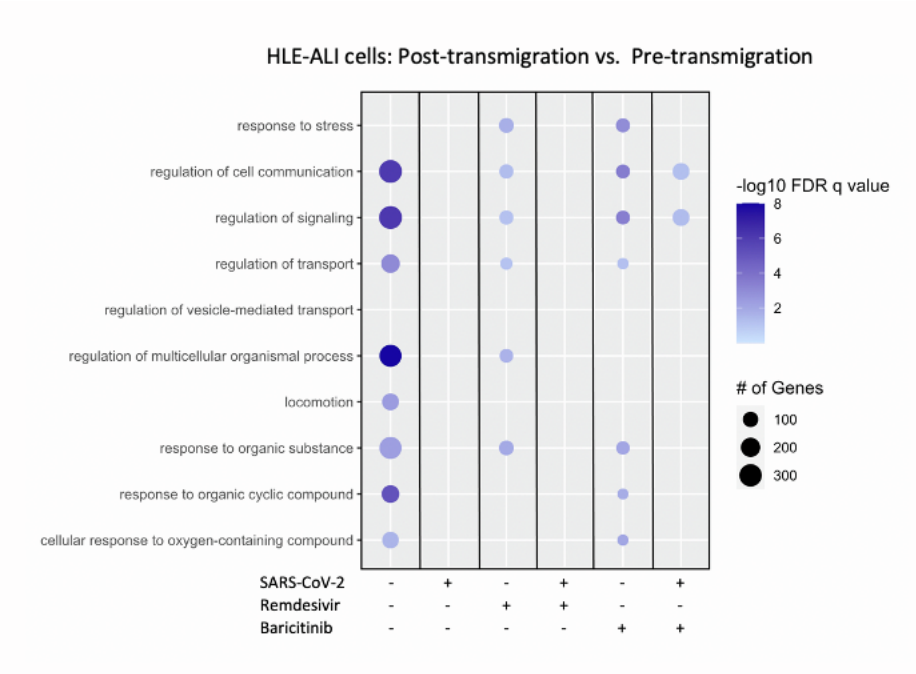

Supplementary Figure 2. Related to Figure 3. Enriched GO terms related to HLE-ALI cells pre- and post- transmigration under each drug and infection condition (n=3 biological replicates).

A

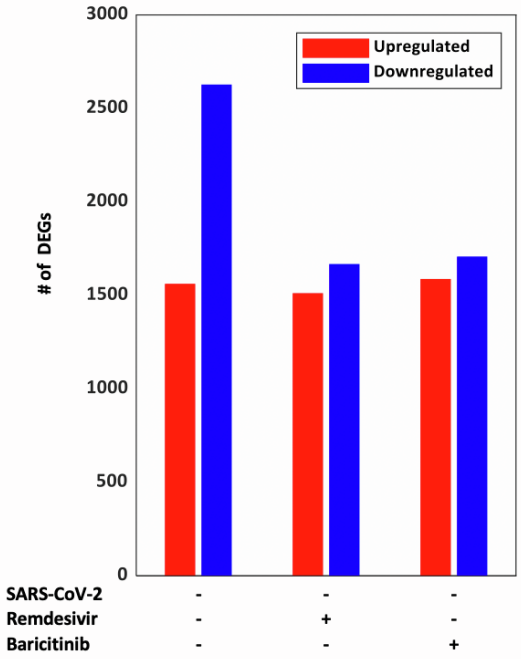

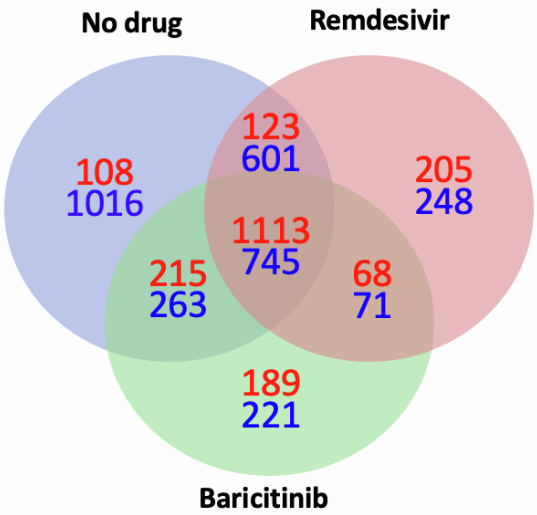

Intersection of DEGs
Post-transmigration
No Infection

B

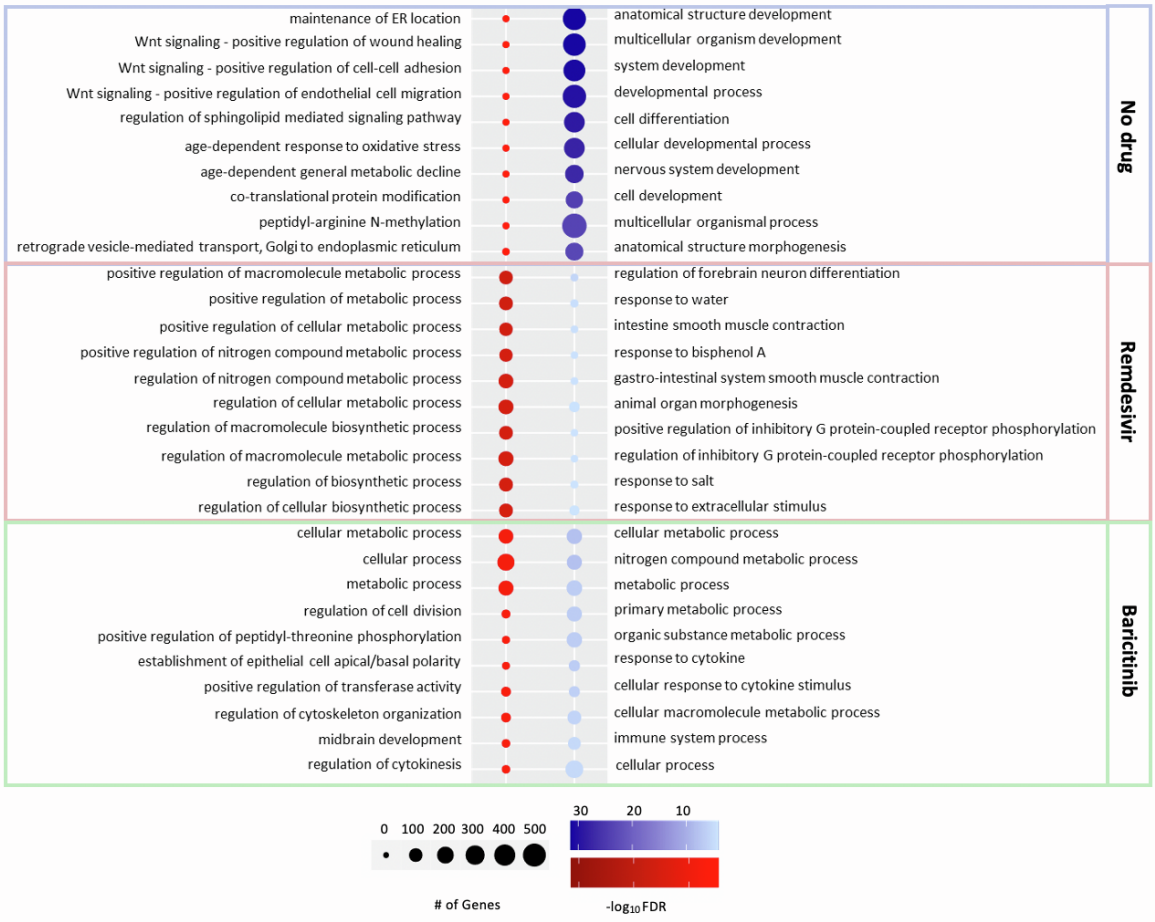

Supplementary Figure 3. Related to Figure 3. (A) Number of upregulated and downregulated DEGs in the RNA-seq data obtained from uninfected HLE-ALI cells after transmigration of monocytes in the presence of either vehicle, remdesivir, or baricitinib (n=3 biological replicates). **(B)** GO processes enriched in uninfected HLE-ALI cells after transmigration of monocytes in the presence of either vehicle, remdesivir, or baricitinib. GO terms were generated using uniquely DEGs between the three conditions.

A

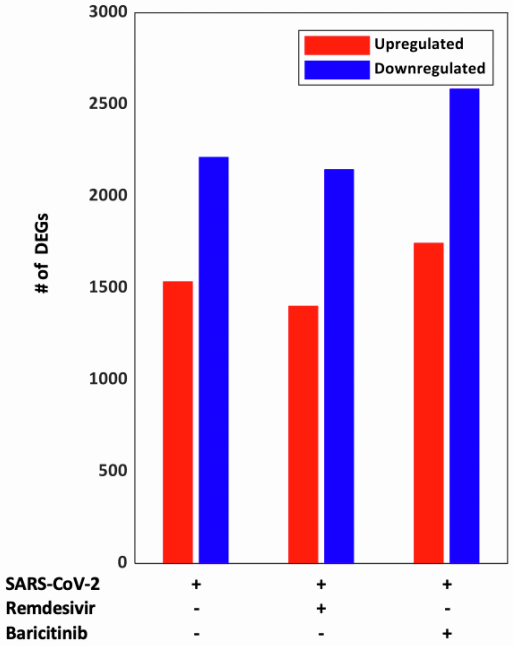

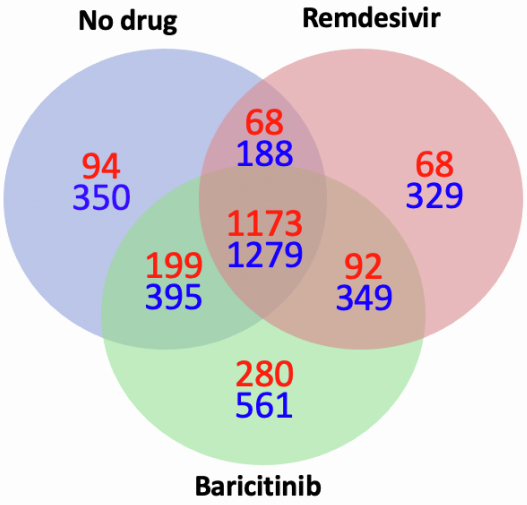

Intersection of DEGs Post-transmigration and Infection

B

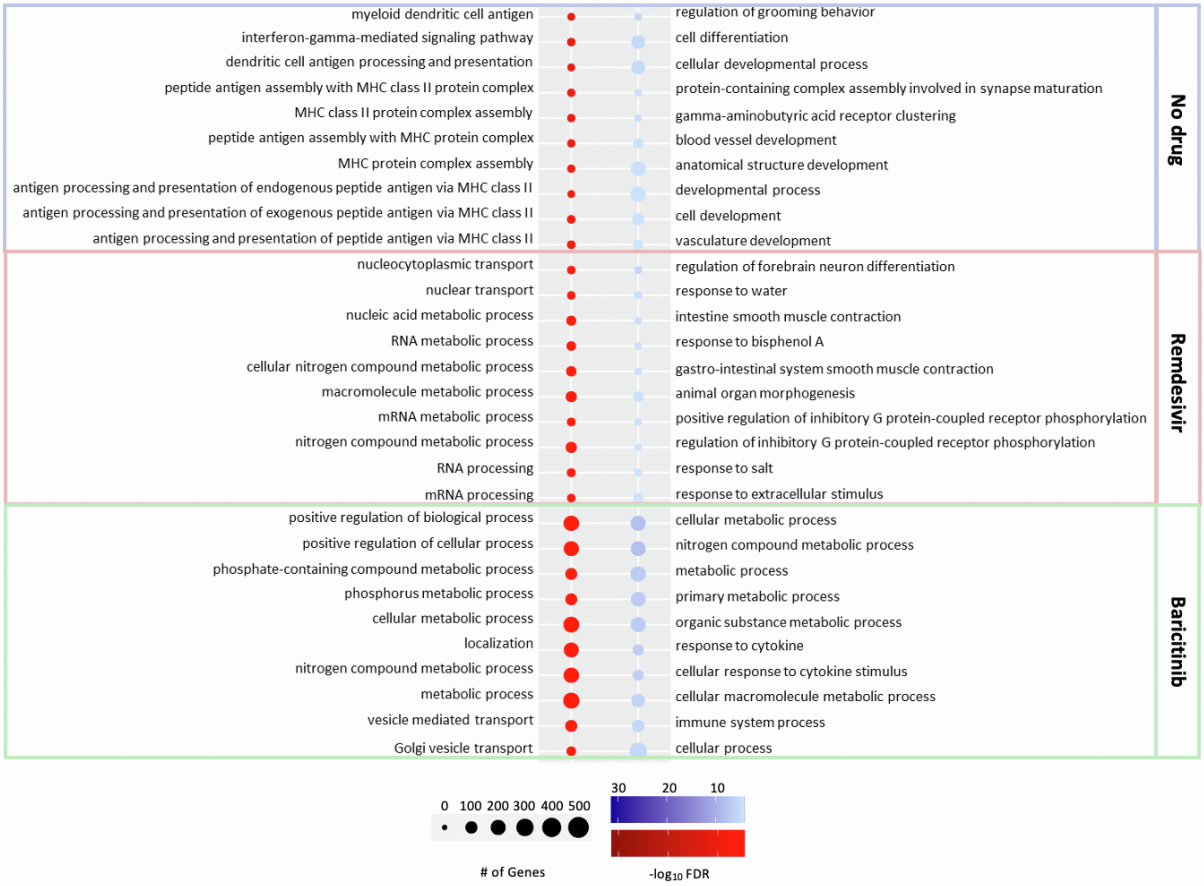

Supplementary Figure 4. Related to Figure 3.(A) Number of upregulated and downregulated DEGs in the RNA-seq data obtained from SARS-CoV-2-infected HLE-ALI cells after transmigration of monocytes in the presence of either vehicle, remdesivir, or baricitinib (n=3 biological replicates). **(B)** GO processes enriched in SARS-CoV-2-infected HLE-ALI cells after transmigration of monocytes in the presence of either vehicle, remdesivir, or baricitinib. GO terms were generated using uniquely DEGs between the three conditions.

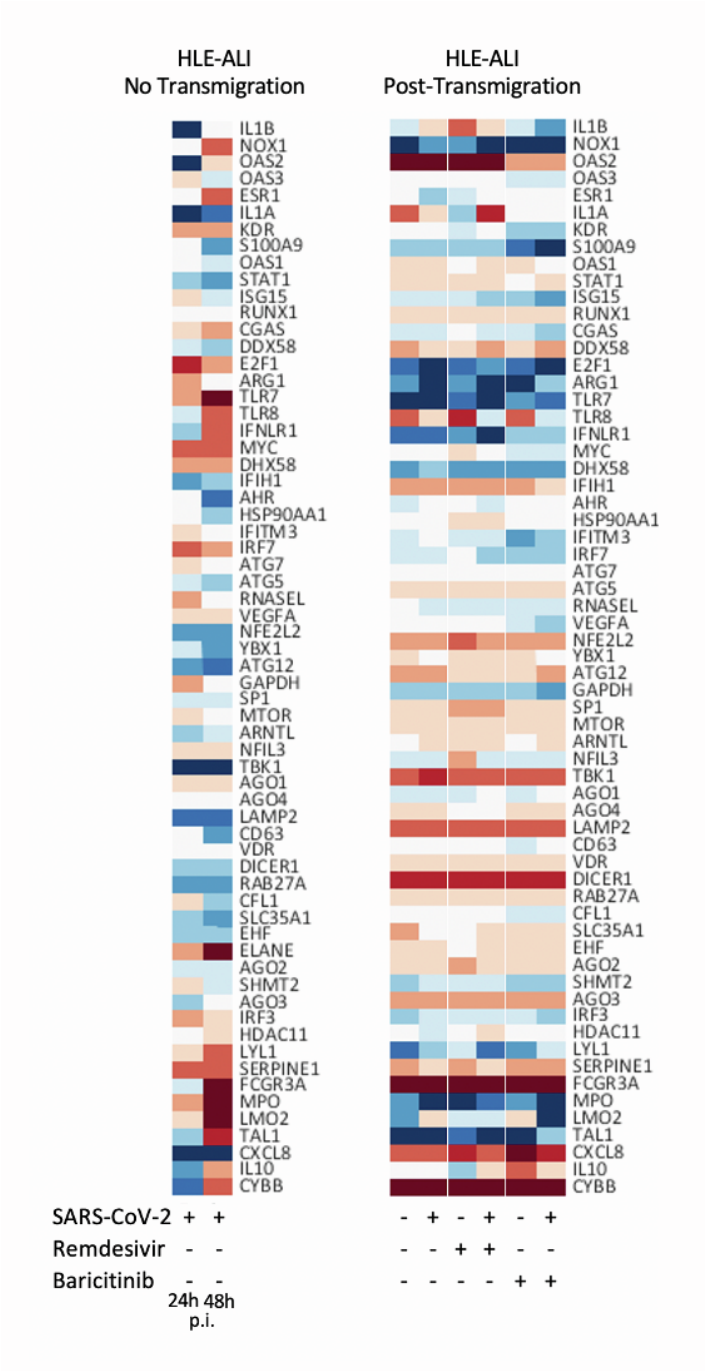

Supplementary Figure 5. Related to Figure 3. Normalized expression values of a set of genes extracted from the RNA-seq data of HLE-ALI cells under each treatment condition (n=3 biological replicates). The set of genes was selected to be the same as the genes selected for qRT-PCR of the monocytes in **Figure 3B.** If a gene was not identified in the RNA-seq data of HLE-ALI cells, it was not listed here.

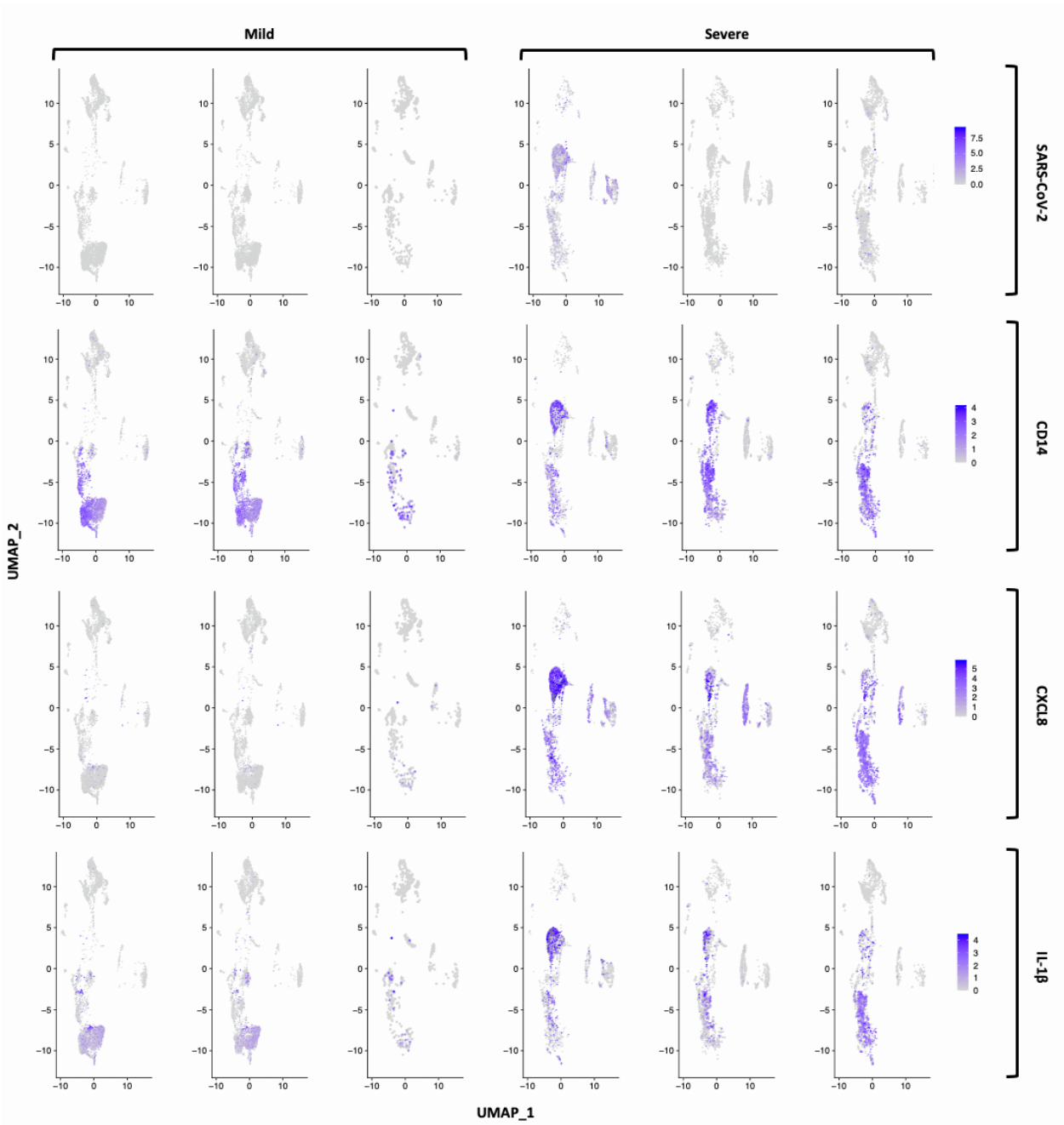

Supplementary Figure 6. Related to Figure 4. Individual UMAPs of scRNA-seq data of BALF from six patients hospitalized with either mild (n=3) or severe (n=3) COVID-19. Original scRNA-seq data is publicly available under accession code GSE145926 (Liao et al., 2020).

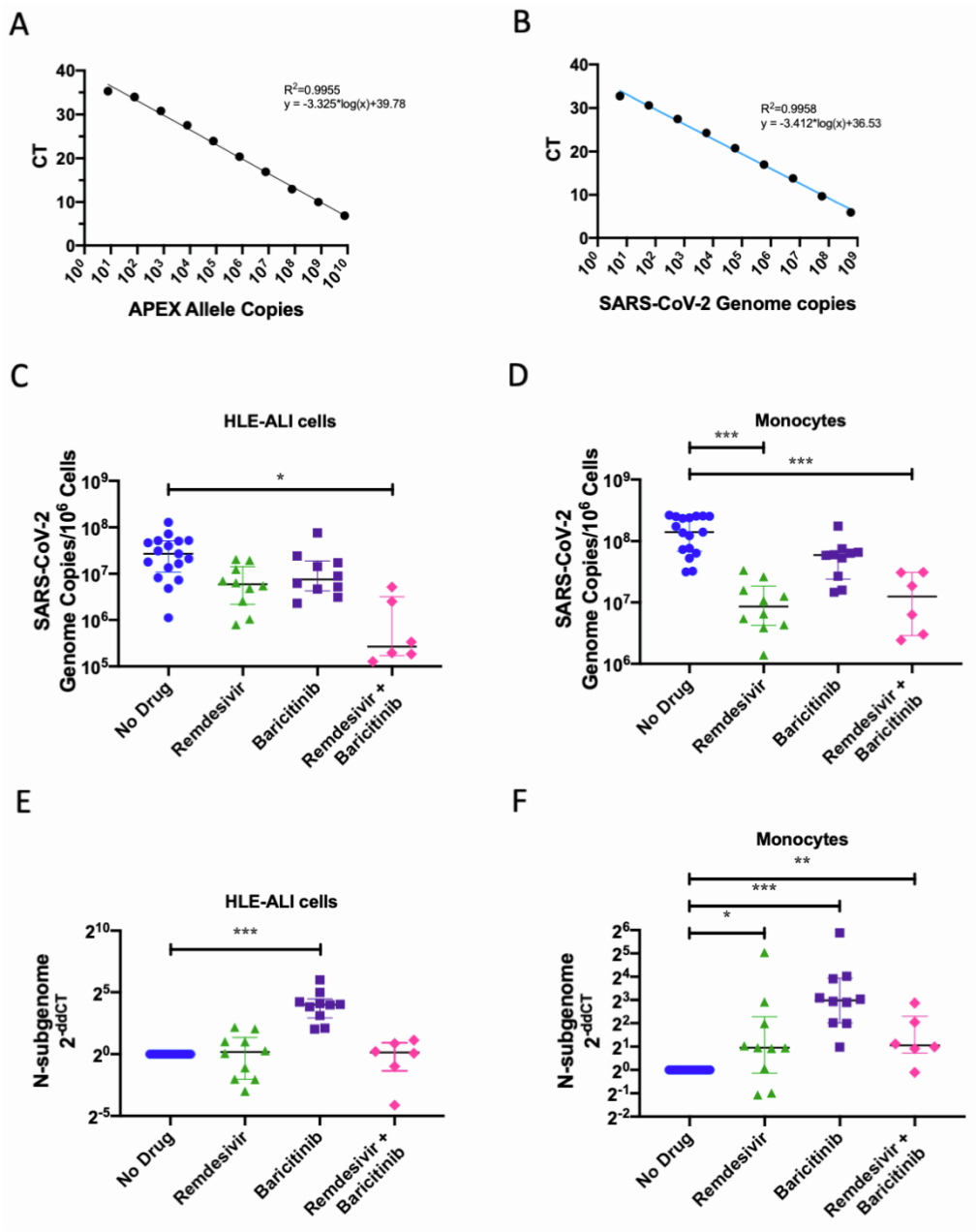

Supplementary Figure 7. Related to Figure 5. SARS-CoV-2 genome copies in each compartment relative to cell number and N-subgenome calculations. (A) In order to calculate cell number a standard curve was used to estimate the number of alleles of APEX present **(see Supplementary Tables 9 and 10)**. This number was transformed by the following calculation to obtain an estimate for cell number: (calculated gene copies) / 2*dilution factor **(B)** A standard curve was generated to calculate the total number of SARS-CoV-2 genome copies

(see Supplementary Tables 9 and 10). (C, D) Calculated SARS-CoV-2 genome copies in each cell was normalized by dividing by the number of cells present. **(E)** Primers aligning to the N-subgenome were used to quantify the replication competency of the virus. Data were normalized using the delta delta Ct method to 18S rRNA **(see Supplementary Tables 9 and 10)** (n=17 for the no drug condition, n=10 for the baricitinib and remdesivir alone conditions, and n=6 for the combined baricitinib and remdesivir conditions). All statistics were calculated using the Mann-Whitney U-test in Prism. * $p<0.05$, ** $p<0.01$, ***$p<0.001$.

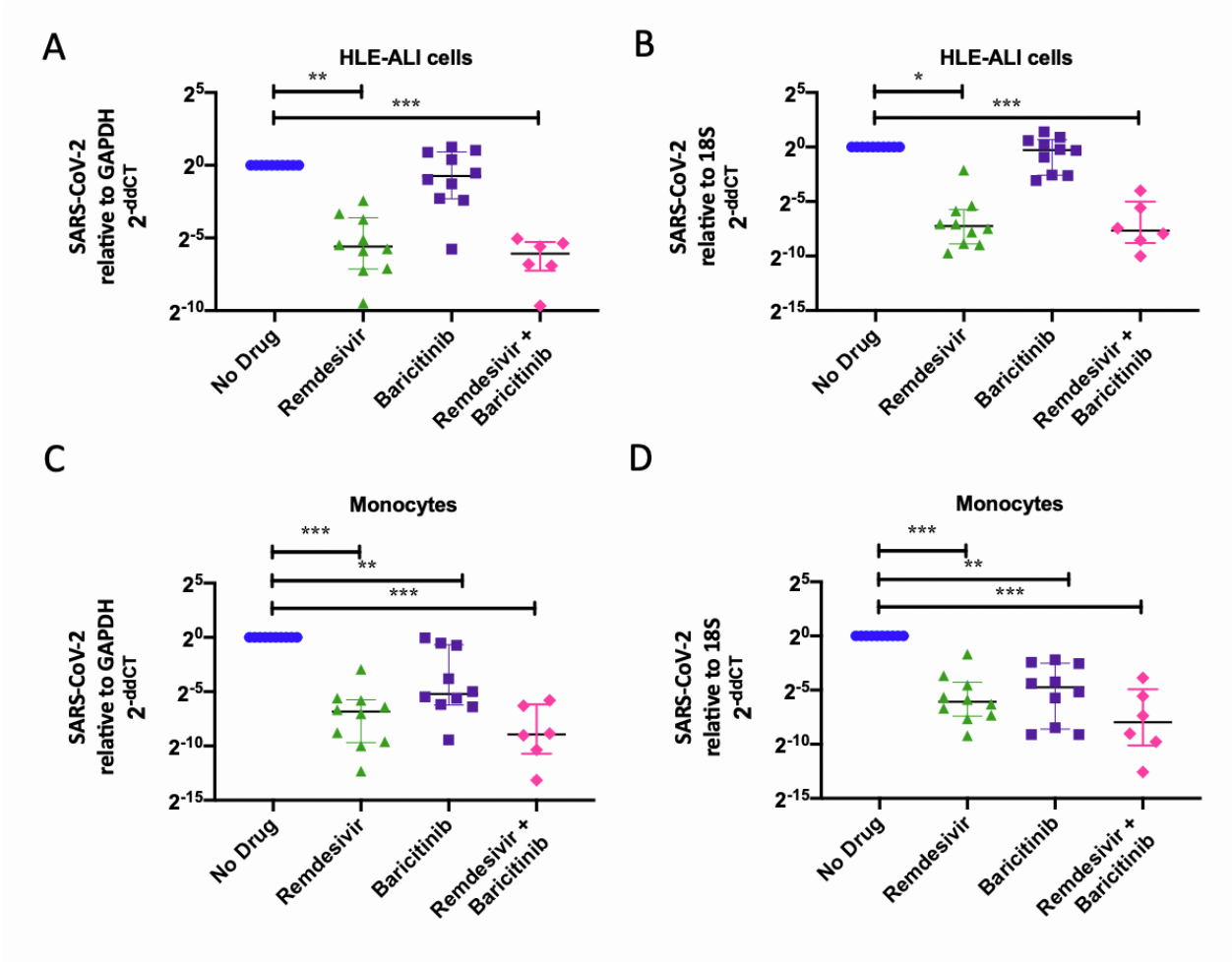

Supplementary Figure 8. Related to Figure 5. (A-D) Calculated SARS-CoV-2 genome copies in each condition was normalized to either GAPDH **(A, C)** or 18S rRNA **(B, D)** in HLE-ALI cells **(A, B)** or monocytes **(C, D)** using the delta delta Ct method **(see Supplementary Tables 9 and 10)** (n=10 for the no drug condition and the baricitinib and remdesivir alone conditions, and n=6 for the combined baricitinib and remdesivir conditions). All statistics were calculated using the Mann-Whitney U-test in Prism. * $p<0.05$, ** $p<0.01$, ***$p<0.001$.

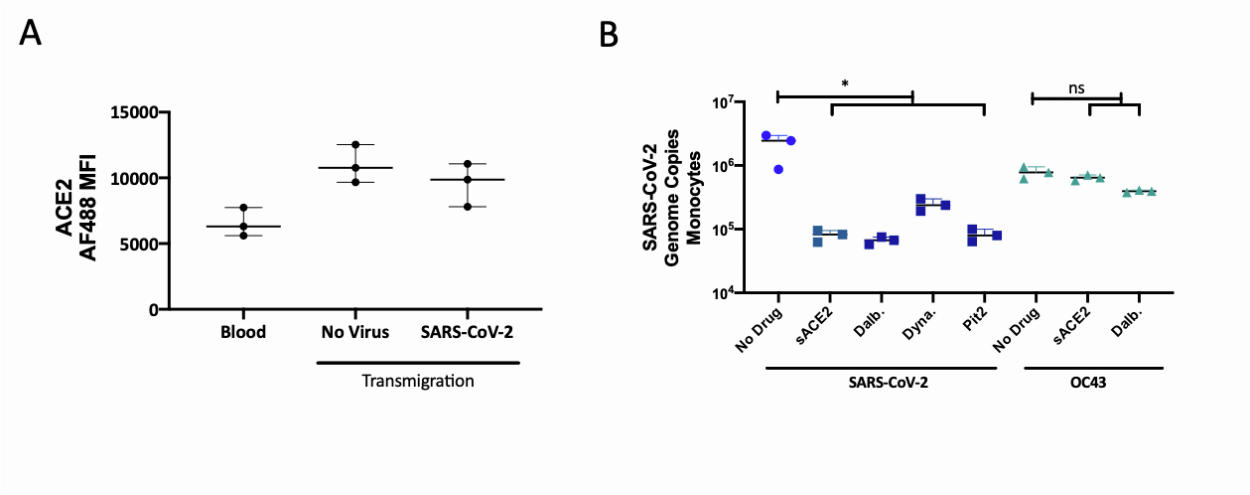

Supplementary Figure 9. Related to Figure 5. (A) Purified blood monocytes before and after transmigration across HLE-ALI cells with or without infection with SARS-CoV-2 were stained for the presence of surface ACE2 and ten analyzed by flow cytometry (n=3 biological replicates). **(B)** Monocytes were transmigrated across HLE-ALI cells infected with either SARS-CoV-2 or OC43. In the apical fluid were soluble ACE2 (200 µg/mL), dalbavancin (1 µM), dynasore (80 µM) or pitstop2 (15 µM) (n=3 biological replicates). Statistics were calculated using a Mann-Whitney U-test in Prism. * $p<0.05$, ** $p<0.01$, ***$p<0.001$.

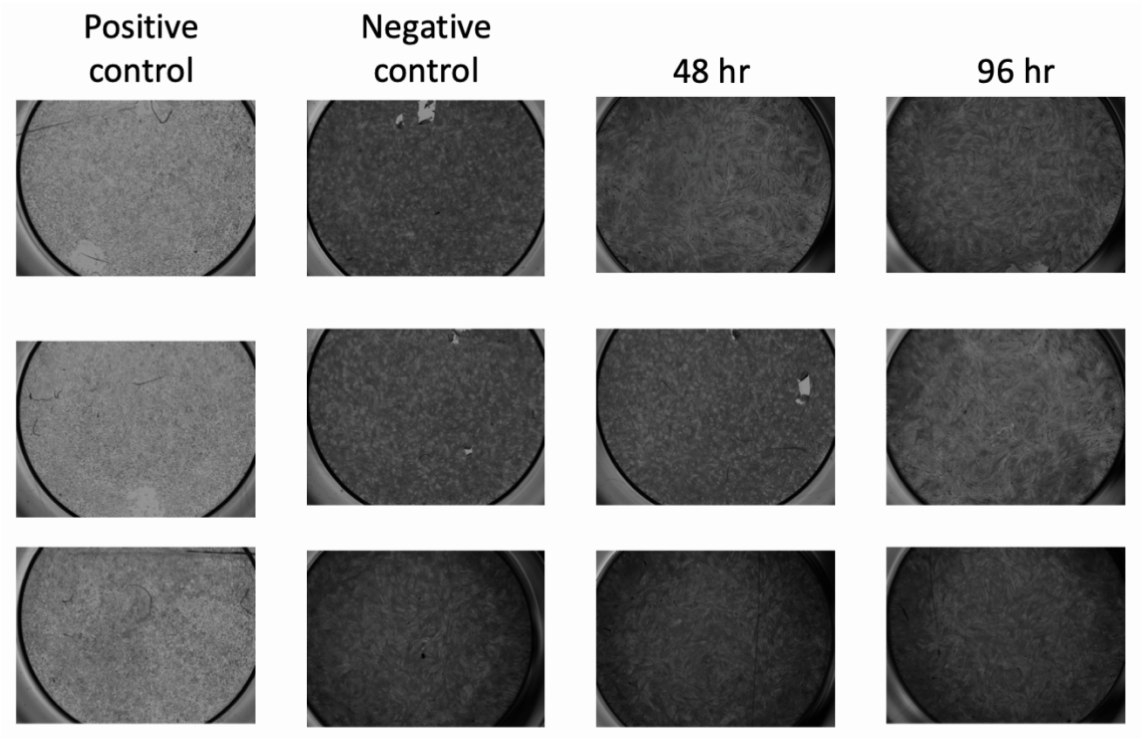

Supplementary Figure 10. Related to Figure 6. Extracellular fluid from cultures of SARS-CoV-2 infected transmigrated monocytes was layered onto VeroE6 cells to perform a plaque assay. The positive control was the direct application of 2.5 x 10^4 genome copies of SARS-CoV-2 to the cells.

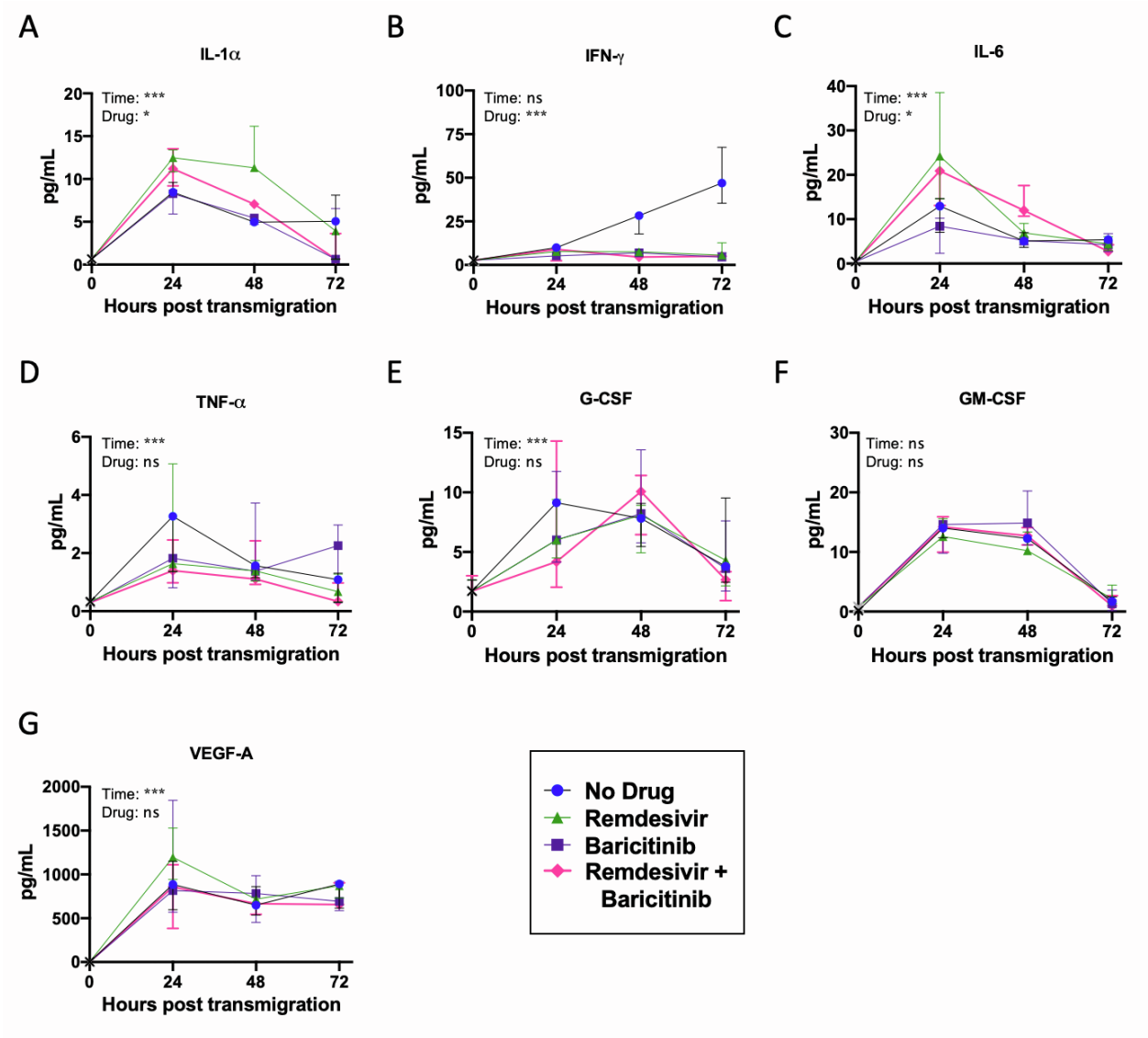

Supplementary Figure 11. Related to Figure 6. Inflammatory mediators from each of the monocyte treatment conditions were quantified using an electrochemiluminescent assay from n=3 biological replicates. All statistics were calculated with a two-way ANOVA, main effects model in Prism with Geisser-Greenhouse correction applied. * $p<0.05$, ** $p<0.01$, ***$p<0.001$. Shown are median and interquartile range.